Cell PRESS

Open ACCESS

Cell Reports

Report

Marburgvirus Hijacks Nrf2-Dependent Pathway by Targeting Nrf2-Negative Regulator Keap1

Audrey Page,[1] Valentina A. Volchkova,[1] Saint Patrick Reid,[1,2] Mathieu Mateo,[1] Audrey Bagnaud-Baule,[1] Kirill Nemirov,[1] Amy C. Shurtleff,[2] Philip Lawrence,[1] Oliver Reynard,[1] Michele Ottmann,[1] Vincent Lotteau,[3] Shyam S. Biswal,[4] Rajesh K. Thimmulappa,[4] Sina Bavari,[2] and Viktor E. Volchkov[1,*]

[1]Molecular Basis of Viral Pathogenicity, Centre International de Recherche en Infectologie (CIRI), INSERMU1111-CNRSUMR5308, Université de Lyon, Université Claude Bernard Lyon1, Ecole Normale Supérieure de Lyon, Lyon 69007, France

[2]United States Army Medical Research Institute of Infectious Diseases, 1425 Porter Street, Fort Detrick, Frederick, MD 21702-5011, USA

[3]IMAP team, CIRI, Lyon 69007, France

[4]Department of Environmental Health Sciences, Bloomberg School of Public Health, Johns Hopkins University, Baltimore, MD 21205, USA

*Correspondence: viktor.volchkov@inserm.fr

http://dx.doi.org/10.1016/j.celrep.2014.02.027

SUMMARY

Marburg virus (MARV) has a high fatality rate in humans, causing hemorrhagic fever characterized by massive viral replication and dysregulated inflammation. Here, we demonstrate that VP24 of MARV binds Kelch-like ECH-associated protein 1 (Keap1), a negative regulator of nuclear transcription factor erythroid-derived 2 (Nrf2). Binding of VP24 to Keap1 Kelch domain releases Nrf2 from Keap1-mediated inhibition promoting persistent activation of a panoply of cytoprotective genes implicated in cellular responses to oxidative stress and regulation of inflammatory responses. Increased expression of Nrf2-dependent genes was demonstrated both during MARV infection and upon ectopic expression of MARV VP24. We also show that Nrf2-deficient mice can control MARV infection when compared to lethal infection in wild-type animals, indicating that Nrf2 is critical for MARV infection. We conclude that VP24-driven activation of the Nrf2-dependent pathway is likely to contribute to dysregulation of host antiviral inflammatory responses and that it ensures survival of MARV-infected cells despite these responses.

INTRODUCTION

Marburgvirus (MARV) causes lethal hemorrhagic fever in humans (Ligon, 2005), while there is currently no vaccine or approved treatment. Fatal MARV infection involves massive disseminated viral replication and host immune dysregulation with uncontrolled cytokine secretion (for review, see Mohamadzadeh, 2009) and a septic-shock-like syndrome (Mahanty and Bray, 2004; Mehedi et al., 2011).

Of seven MARV structural proteins (Feldmann and Klenk, 1996), NP, VP30, VP35, and RNA-dependent RNA polymerase L are required for RNA replication and transcription (Feldmann et al., 1993). A single-surface glycoprotein, GP, mediates viral entry (Volchkov et al., 2000; Will et al., 1993). The matrix protein VP40 is involved in virus assembly and budding and antagonizes interferon (IFN) signaling (Valmas and Basler, 2011; Valmas et al., 2010). Little is known about viral protein VP24 function (Bamberg et al., 2005). However, a recent mass spectrometry screen revealed that filoviral VP24 proteins might have multiple potential cellular partners (Pichlmair et al., 2012). In the case of Ebolavirus (EBOV), another member of the Filoviridae family, VP24 has been implicated in virus budding (Huang et al., 2002) and nucleocapsid assembly (Mateo et al., 2011a) and is an important pathogenicity factor, antagonizing IFN signaling and aiding adaptation to new animal hosts (Mateo et al., 2010, 2011b; Reid et al., 2006, 2007). Although causing apparently similar hemorrhagic disease in humans, MARV and EBOV appear to use different proteins and strategies to prevail over a host's defense system. This raises important questions concerning the role of MARV VP24; specifically, what are the cellular partners of MARV VP24, and what are its potentially novel functions in MARV replication that may underlie its potent pathogenicity?

The cellular Nrf2 (nuclear factor erythroid 2-related factor 2)-dependent pathway protects against environmental insults and oxidative stress (Ma, 2013; Thimmulappa et al., 2006) and maintains cellular redox balance by regulating endogenous antioxidants, phase II detoxification enzymes, and other defensive proteins via antioxidant response elements (AREs) in target gene promoters (Jaiswal, 2004). Under quiescent conditions, Nrf2 is cytoplasmic and bound to its repressor Keap1 (Kelch-like ECH-associated protein 1) (Itoh et al., 1999). Keap1 constitutively targets Nrf2 for ubiquitination and thus proteasomal degradation by acting as a substrate adaptor for the Cul3-based E3 ubiquitin ligase complex (Furukawa and Xiong, 2005; Kobayashi et al., 2004). Under oxidative stress, Keap1 loses its ability to repress Nrf2 via its proteosomal degradation (Kobayashi et al., 2006). Nrf2 then translocates into the nucleus where it heterodimerizes with Maf proteins (Motohashi et al., 2004), binds ARE-containing promoters, resulting in enhanced expression of a range of antioxidant, cytoprotective genes (Itoh et al., 1999). Well-characterized Nrf2-dependent genes include Heme Oxygenase-1 (HO1), NAD(P)H dehydrogenasequinine-1 (NQO1), Glutamate Cysteine Ligase (GCL), and Glutathione S-transferase A1 (GSTA1) (Jaiswal,

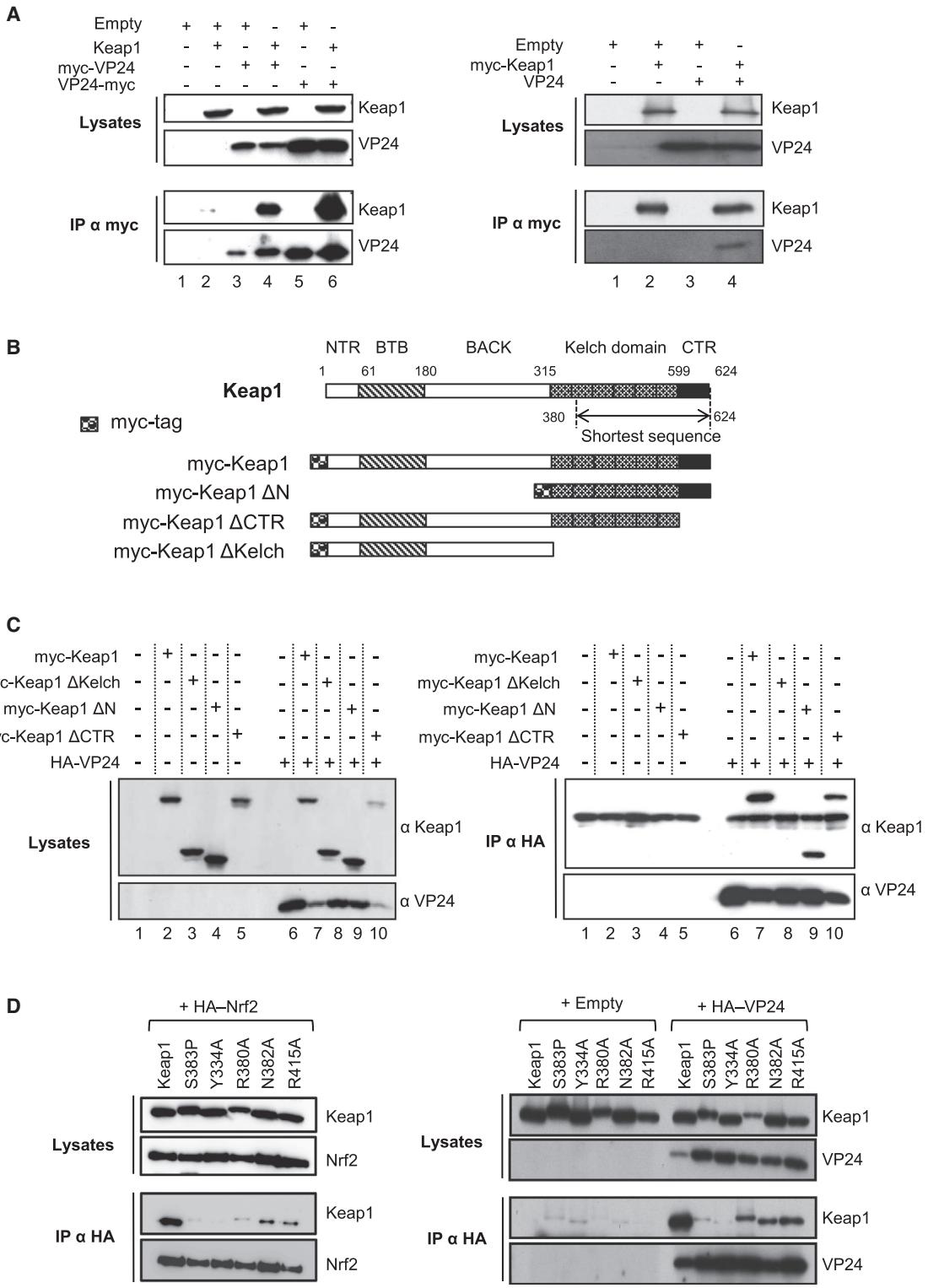

Figure 1. MARV VP24 Interacts with Keap1

(A) Reciprocal immunoprecipitations of MARV VP24 and Keap1. N- and C-terminal myc-tagged VP24 were coexpressed with Keap1 (left panels). Twenty-four hours posttransfection (p.t.), cell lysates were analyzed by western blot and coprecipitation using myc antibody followed by western blot using Keap1 and VP24 antibodies. Right panels: myc-tagged Keap1 and nontagged VP24 were coexpressed. Cell lysates were assayed for protein expression and coprecipitation using myc antibody followed by western blot using Keap1 and VP24 antibodies.

(legend continued on next page)

2004). The Nrf2 pathway has also been implicated in innate immunity by regulating cellular inflammation responses (Rushworth et al., 2008; Thimmulappa et al., 2006). Recent evidence suggests that Nrf2 acts in viral infection, though the underlying molecular mechanisms remain poorly understood (Burdette et al., 2010; Carvajal-Yepes et al., 2011; Cho et al., 2009; González-Gallego et al., 2011; Zhang et al., 2009).

We now uncover a cellular partner of MARV VP24 and link this interaction to the host response. Precisely, we show that MARV hijacks the Nrf2-antioxidant defense system and that viral protein VP24 binds Keap1 via its Kelch domain, liberating Nrf2 from Keap1 control, and activating the Nrf2 pathway. Activation of Nrf2 was observed upon transient expression of VP24 and during MARV infection. Experiments in Nrf2$^{-/-}$ mice further highlight the significance of the Nrf2 pathway for Marburgvirus replication and pathogenicity.

RESULTS

MARV VP24 Binds Keap1 through Its Kelch Domain

To identify cellular partners of MARV VP24, we used a yeast double-hybrid screening approach, fusing VP24 to a Gal4DNA binding domain and cellular proteins encoded by a human spleen cDNA library to a Gal4-activation domain. VP24 of EBOV, which was previously shown to interact with cellular karyopherins (Reid et al., 2006, 2007), was used as control. As expected, the cDNAs encoding for karyopherin α1, α5, and α6 were retrieved in control experiments, thus validating the screening approach. However, none of the karyopherins were among those cellular proteins found to interact with MARV VP24. From 125 yeast colonies, 60 contained sequences corresponding to cellular Keap1, the cytoplasmic repressor of Nrf2 (Table S1). Among these 60 cDNAs, the shortest fragment encoded the 244 carboxy-terminal amino acids of Keap1. To confirm an interaction between the two proteins, amino- and carboxy-terminal-tagged VP24 of MARV (myc-VP24 and VP24-myc) were coexpressed with human Keap1 in 293T cells, and lysates were subjected to immunoprecipitation with myc antibodies followed by western blot analysis using Keap1 and VP24 antibodies. Both myc-tagged VP24 constructs coprecipitated plasmid-expressed Keap1 (Figure 1A, left panel, compare lanes 4 and 6 to lane 2). The reciprocal immunoprecipitation confirmed an interaction between the two proteins, where nontagged VP24 coprecipitated a myc-tagged Keap1 (Figure 1A, right panel, lanes 3 and 4). As expected, nontagged Keap1 and VP24 were not precipitated by myc antibodies when these proteins were expressed without myc-tagged partners (Figure 1A, left panel, lane 2, and right panel, lane 3). We also demonstrated that endogenous Keap1 could be precipitated by MARV VP24 (Figure S1).

Resolution of the 3D structure of Keap1 has provided insights into the functional domains of this protein (Ogura et al., 2010). It was important to identify which domain of Keap1 is responsible for interaction with MARV VP24. The data obtained through yeast screening suggested that the carboxy-terminal end of Keap1 is likely to be involved in VP24 binding. To confirm this, a set of myc-tagged Keap1 deletion mutants was generated (Figure 1B). Keap1 deletion mutants myc-tagged at the amino-terminal end and hemagglutinin (HA)-tagged VP24 were coexpressed in 293T cells, and the interaction between the proteins was analyzed by coprecipitation using HA antibodies (Figure 1C). Keap1 deletion mutants lacking either the amino terminal part (ΔN) or carboxy-terminal region (ΔCTR) were coprecipitated with VP24 in a manner similar to that of the full-length Keap1 (Figure 1C, right panel, compare lanes 9 and 10 to lane 7). However, a Keap1 mutant lacking the double glycine Kelch-repeat domain (ΔKelch) completely lost the capacity to bind VP24 (Figure 1C, right panel, lane 8). Because the Kelch domain has been described as the Nrf2 binding site, we investigated whether Keap1 mutants defective for Nrf2 binding interact with MARV VP24 (Figure 1D). To address this question, a previously described set of Keap1 Kelch domain mutants was generated (Li et al., 2004a; Lo et al., 2006). First, we coexpressed myc-tagged Keap1 mutants with HA-tagged Nrf2 and analyzed interaction by immunoprecipitation using HA antibodies. As expected, mutants containing alanine substitutions (Y334A, R380A, N382A, and R415A) and Keap1 mutant S383P possessed a reduced capacity to interact with Nrf2 (Figure 1D, left panel). Myc-tagged Keap1 mutants and HA-tagged VP24 were then coexpressed in 293T cells, and lysates were analyzed for interaction between Keap1 and MARV VP24. When compared to the wild-type protein, all Keap1 mutants showed a decrease in their abilities to bind MARV VP24 (Figure 1D, right panel). Similar to the results obtained with Nrf2, Keap1 mutants S383P and Y334A almost completely lost the ability to bind VP24, whereas others showed a reduction in binding efficiency. These results confirmed that the VP24 binding site is located within the Keap1 Kelch domain and that the binding sites of Nrf2 and VP24 are likely to overlap.

Next, we studied the interaction between Keap1 and MARV VP24 using immunofluorescent analysis. Vero E6 cells were transfected with plasmids expressing the proteins either alone or in tandem, and their intracellular distribution was analyzed (Figure 2). Notably, MARV VP24 expressed in the absence of other ectopic proteins displayed a spotted perinuclear pattern (Figure 2, top panels). Conversely, consistent with previous reports, Keap1 expressed alone showed a homogenous cytoplasmic distribution (Kang et al., 2004). Strikingly, intracellular localization of both proteins was dramatically altered when

(B) Schematic representation of Keap1 domain structure and Keap1 deletion mutants. Keap1 is composed of an Amino Terminal Region (NTR), a Bric-a-brac, Tramtrack, Broad-complex domain (BTB), a BACK domain, a Kelch domain, and a C-terminal Region (CTR). The shortest Keap1 cDNA retrieved in yeast double-hybrid screen encodes 244 aa from the carboxy-terminal end of Keap1 (380–624 aa). All Keap1 deletion mutants were myc tagged at the amino terminal end.
(C) Deletion of Kelch domain prevents MARV VP24 binding. Keap1 deletion mutants were either expressed alone or coexpressed together with HA-tagged VP24. Cells were analyzed 24 hr p.t. by western blot (left panels) and by coimmunoprecipitation using HA antibodies followed by western blot with VP24 and Keap1 antibodies (right panels).
(D) Nrf2 and MARV VP24 bind Keap1 in a similar manner. Myc-tagged Keap1 Kelch domain mutants deficient in Nrf2 binding were expressed either alone or together with HA-tagged VP24 (left panels) or with HA-tagged Nrf2 (right panels). Twenty four hours p.t., lysates were analyzed by western blotting using Keap1 and VP24 or HA and myc antibodies (upper panels), or by coimmunoprecipitation using HA antibodies followed by western blot with VP24 and Keap1 antibodies (bottom panels).

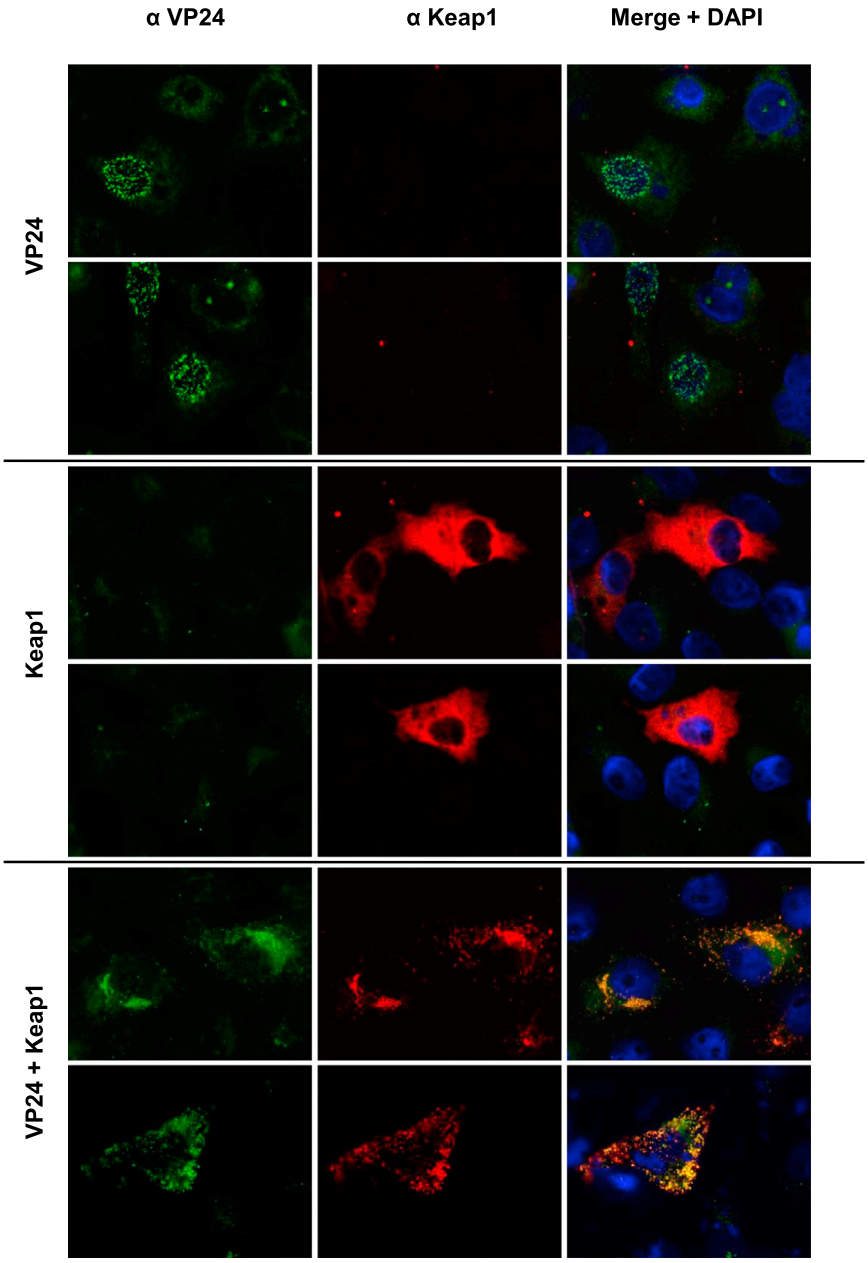

Figure 2. Coexpression of MARV VP24 and Keap1 Results in Intracellular Relocalization of Both Proteins and Their Colocalization

MARV VP24 and Keap1 were expressed alone or in combination in Vero E6 cells. Sixteen hours p.t., cells were fixed using acetone/methanol and subjected to immunofluorescence analysis using VP24 and Keap1 antibodies. Nuclei were stained with DAPI.

they were coexpressed. In effect, both proteins colocalized and could be seen as patch-like aggregates distributed throughout the cytoplasm (Figure 2, bottom panels).

MARV VP24 Induces Nrf2 Activation

Keap1 represses Nrf2 activity by binding cytosolic Nrf2, facilitating its ubiquitination and promoting proteasomal-mediated degradation (Itoh et al., 1999). Based on our results, we hypothesized that VP24 binding to Keap1 would impair Keap1-mediated negative regulation of Nrf2. To verify this, we used a gene reporter assay to monitor the activity of firefly luciferase expressed under the control of two different Nrf2-dependent ARE promoters corresponding to HO1 and NQO1 genes. 293T cells were transfected with combinations of the following plasmids: pHHO1-ARE-Luc or pmNQO1-ARE-Luc and phCMV-Nrf2, pSPORT6-Keap1, p-RL-TK-Luc, and phCMV-MARV-VP24 as indicated (Figures 3A and 3B). Firefly luciferase activity was normalized to renilla luciferase expressed from pRL-TK plasmid that served as a control. Firefly luciferase activity markedly increased in cells expressing Nrf2. This induction was substantially reduced upon coexpression of Nrf2 and Keap1. Importantly, expression of MARV-VP24 restores firefly luciferase activity inhibited by Keap1 for both HO1 and NQO1 ARE-Luc reporters, and this effect is VP24 dose dependent. Increased reporter gene expression suggests that Keap1 loses its ability to negatively regulate Nrf2 function upon MARV VP24 binding, allowing free Nrf2 to activate transcription of Nrf2-dependent genes.

Activation of the Nrf2 pathway by MARV VP24 was further evaluated by analysis of Nrf2-dependent gene expression. Data obtained show that MARV VP24 is able to alleviate Keap1-mediated inhibition of both NQO1 and HO1 expression in a VP24 dose-dependent manner (Figures 3A and 3B, right panels). Next, it was important to demonstrate that MARV VP24 can also affect the expression of Nrf2-dependent genes when neither Nrf2 nor Keap1 are overexpressed. 293T cells were transfected with different amounts of phCMV-MARV-VP24 or an empty vector and expression of NQO1 was assayed (Figure S2). This analysis showed an increase in NQO1 expression in VP24-transfected cells in a dose- and time-dependent manner, whereas very little NQO1 was detected in cells transfected either with an empty vector or phCMV-EBOV-VP30 used as control. To provide mechanistic proof of the ability of VP24 to release Nrf2 from its cytoplasmic association with Keap1, we monitored the intracellular localization of Nrf2 in the presence of MARV VP24 by immunofluorescence (Figure 4). Vero E6 cells were transfected with plasmids expressing Nrf2 alone, or Nrf2 with Keap1, or Nrf2, Keap1, and VP24 together.

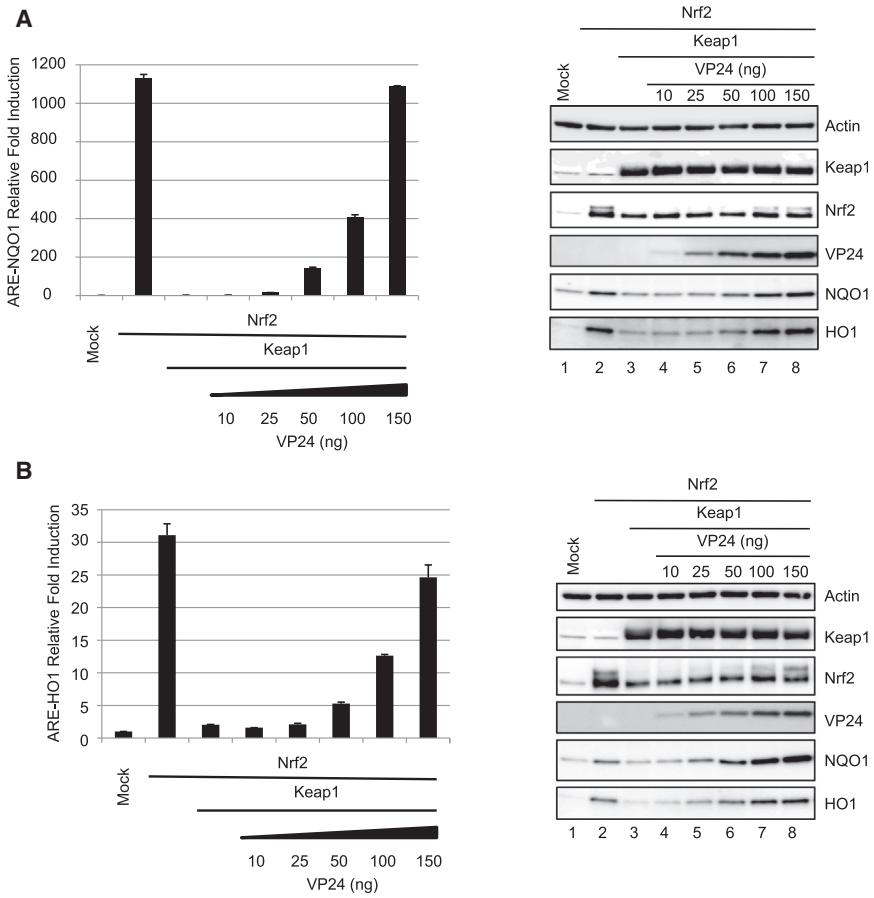

Figure 3. MARV VP24 Induces Nrf2 Activation and Expression of Nrf2-Dependent Genes

Reporter gene assay. Cells were transfected with the following plasmids: phCMV (Mock), phCMV-MARV-VP24 (VP24), pSPORT6-Keap1 (Keap1), phCMV-Nrf2 (Nrf2), pHHO1-ARE-Luc (left panel) or pmNQO1-ARE-Luc (right panel), and pRLTk-Luc. Different amounts of phCMV-MARV VP24 were used as indicated. Twenty-four hours later, cells were lysed, and firefly and renilla luciferase activities were assayed. Firefly luciferase activity was normalized to renilla luciferase activity. Normalized values are shown relative to values obtained from cells transfected with control plasmid phCMV (A and B, left panels). The graph represents the average values from three different experiments; error bars show SEM (A and B, right panels). Cell lysates were analyzed by western blot using VP24, Nrf2, Keap1, HO1, NQO1, and actin antibodies.

Nrf2 expressed alone was found in the nuclei, whereas coexpression of Nrf2 and Keap1 resulted in a predominantly cytoplasmic localization of Nrf2. Coexpression of Nrf2 and Keap1 together with MARV VP24 resulted in relocalization of Nrf2 from the cytoplasm into the nuclei confirming that MARV VP24 releases Nrf2 from Keap1 binding. Competition between Nrf2 and VP24 for Keap1 binding was confirmed by IP experiments (Figure S3). An increase in levels of VP24 expression causes a simultaneous increase in the amount of Keap1-precipitated VP24 and a reduction in the amount of Keap1-precipitated Nrf2.

Marburg Viruses Hijack the Cellular Nrf2-Dependent Pathway

We then addressed the importance of the Nrf2 pathway during MARV infection. First, using Vero E6 cells we demonstrated that infection with MARV results in increasing levels of NQO1 over 8 days postinfection (Figure 5A) while causing apparent cytotoxic effects (Figure 5B). Similar results were obtained with 293T cells (Figure S4). Using 293T cells, we also showed that levels of NQO1 increased during the course of infection with live MARV, whereas only low levels of NQO1 could be detected when cells were inoculated with UV-inactivated virus and that an enhanced NQO1 expression correlated with increasing levels of VP24 synthesized during infection (Figure 5C). Remarkably, there was no increase in NQO1 levels when the cells were infected with EBOV whose VP24 does not interact with Keap1 (data not shown). Contrary to MARV, infection with EBOV causes higher and earlier cytotoxicity and results in appearance of reactive oxygen species detected using a fluorescent probe (Figure S5).

To demonstrate that the VP24-driven upregulation of Nrf2 has significance under physiological conditions, we used mice as a model of infection. Adult mice are resistant to Marburgvirus infection. However, passaging of marburgvirus RAVN in mice resulted in a mouse-adapted variant (ma-RAVV) causing lethal disease. Importantly, the disease caused by ma-RAVV resembles that seen in nonhuman primates with MARV and is also characterized by uncontrolled viremia and high viral titers in the liver and other organs in infected animals (Warfield et al., 2009). The ma-RAVV and Nrf2-deficient mice ($Nrf2^{-/-}$) are therefore a suitable model to address the importance of the Nrf2 pathway for replication and pathogenicity of Marburgviruses. Because RAVN VP24 possesses several amino acid changes compared to MARV VP24, we investigated whether RAVN VP24 interacts with Keap1 using a coprecipitation assay. Similar to MARV, RAVN VP24 is able to precipitate Keap1 (Figure 5D). Furthermore both VP24 proteins showed a similar ability to upregulate the Nrf2 pathway with an increase in luciferase activity using an ARE-NQO1-luciferase reporter assay (data not shown). Next, groups of wild-type and $Nrf2^{-/-}$ mice were inoculated intraperitoneally with 1,000 plaque-forming units (pfu) of the ma-RAVV, and animals were monitored daily for the appearance of symptoms. Blood was sampled for virus recovery on day 4 from four animals from each group and from surviving animals on day 9. Wild-type mice uniformly succumbed to infection within 8 days (Figure 5E, left panel) consistently demonstrating typical clinical signs of MARV disease, including ruffled, ungroomed fur, hunched posture, reduced activity, and

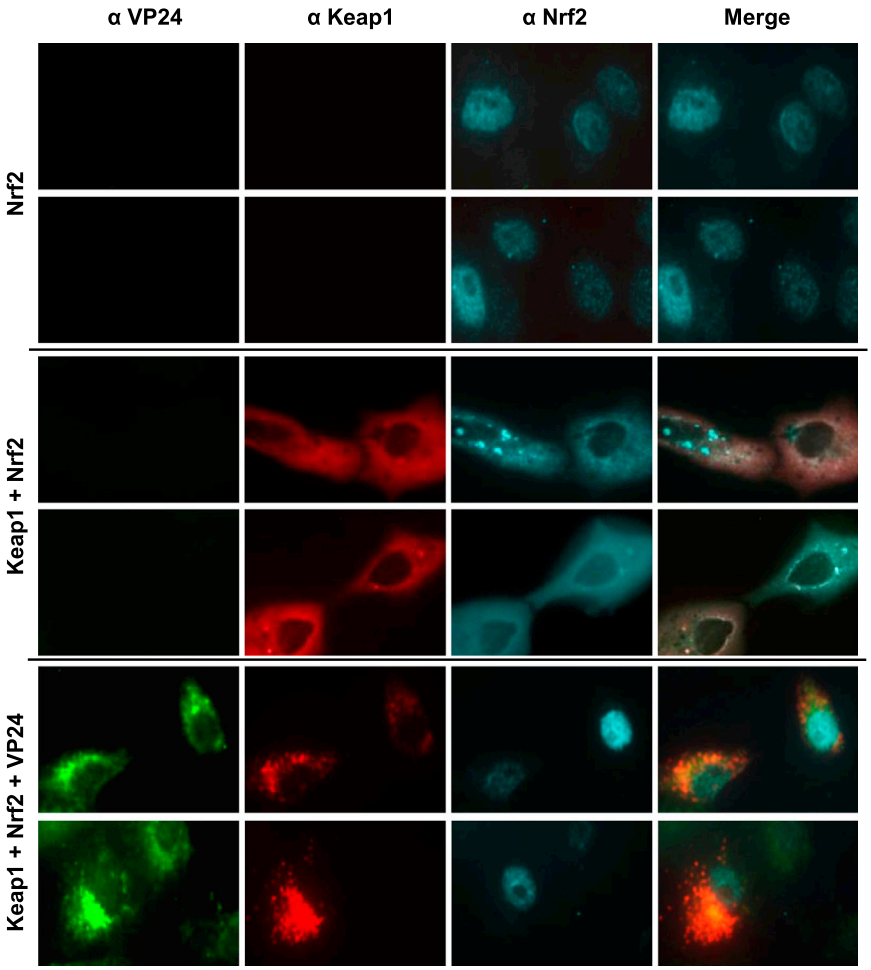

Figure 4. MARV VP24 Releases Nrf2 from Keap1 Control and Facilitates Nrf2 Translocation into the Nuclei

Nrf2, Keap1, and MARV VP24 were expressed in Vero E6 cells alone or in combination as indicated. Sixteen hours posttransfection, cells were fixed using acetone/methanol and subjected to immunofluorescence analysis using VP24, Keap1, and Nrf2 antibodies.

weight loss. In contrast, Nrf2$^{-/-}$ animals proved to be more resistant. Remarkably, all Nrf2$^{-/-}$ animals displayed disease symptoms to varying degrees during the first 6–7 days of infection. The animals that showed greater signs of disease, succumbed to infection. Otherwise, 50% of the animals survived infection, recovered, and appeared to remain healthy throughout the period of observation, which lasted 19 days postinfection (Figure 5E, right panel). These mice appeared to have a smooth, groomed coat, were active, and demonstrated normal posture. On day 4 postinfection, viral titers in the sera of wild-type and Nrf2$^{-/-}$ mice were shown to be lower in the case of Nrf2$^{-/-}$ animals ($5.37 \pm 1 \times 10^5$ versus $1.99 \pm 0.9 \times 10^5$). Strikingly, no infectious virus was detected in the sera of surviving mice on day 9 p.i. In conclusion, both in vitro experiments with live virus and in vivo experiments with Nrf2-deficient mice strongly support the notion that the Nrf2 pathway plays a critical role during Marburgvirus infection and may contribute to high mortality rates.

DISCUSSION

The discovery of host factors involved in Marburg virus replication elucidates the molecular mechanisms underlying pathogenesis, and potentially the cellular pathways hijacked by other highly pathogenic viruses. Our study provides evidence indicating that MARV VP24 plays a critical role during virus replication by binding Keap1, a cytosolic repressor of Nrf2 and modulating the function of the Nrf2-dependent cytoprotective pathway devoted to cellular redox balance (Ma, 2013) and regulation of cellular inflammation responses (Rushworth et al., 2008; Thimmulappa et al., 2007). This VP24 function is of particular interest for filovirus infection because the disease is characterized by dysregulation of inflammatory responses (Baize et al., 2002; Mahanty and Bray, 2004; Mohamadzadeh, 2009; Rubins et al., 2007) and is associated with oxidative stress at viral replication sites (Geisbert et al., 2003; Sanchez et al., 2004).

Here, an interaction between VP24 and Keap1 was revealed using several approaches. Notably, we showed that coexpression of VP24 and Keap1 led to dramatic relocalization of both proteins. We show that MARV VP24 upregulates expression of Nrf2-dependent genes in a dose-dependent fashion by competing for Nrf2 binding sites and preventing Keap1 from suppressing Nrf2. Using a series of Keap1 mutants defective for Nrf2 binding (Li et al., 2004a, 2004b; Lo et al., 2006), we find that Nrf2 and VP24 binding sites overlap. These results correlate well with those using Keap1 deletion mutants to show that MARV VP24 targets the Nrf2 binding site (the Keap1 Kelch domain) and are consistent with interaction results seen in our initial double-hybrid screen.

The structure of the Keap1:Nrf2 complex has been reported (Padmanabhan et al., 2008) indicating that the Keap1 homodimer binds to one Nrf2 molecule via two recognition sites, the DLG and ETGE motifs in the Nrf2 Neh2 domain (Tong et al., 2006). Although Keap1 shares a common binding site for the DLG and ETGE motifs of Nrf2, this dual recognition has physiological relevance (Tong et al., 2007). In the currently accepted hinge-latch model of Keap1 inhibition of Nrf2, Keap1 recruits Nrf2 via the ETGE motif, whereas the DLG motif keeps the molecule in a correct position for ubiquitination. MARV VP24 binding to the Kelch domain would thus interfere with Keap1 binding to both Nrf2 sites, thus providing a mechanism of the Nrf2 pathway

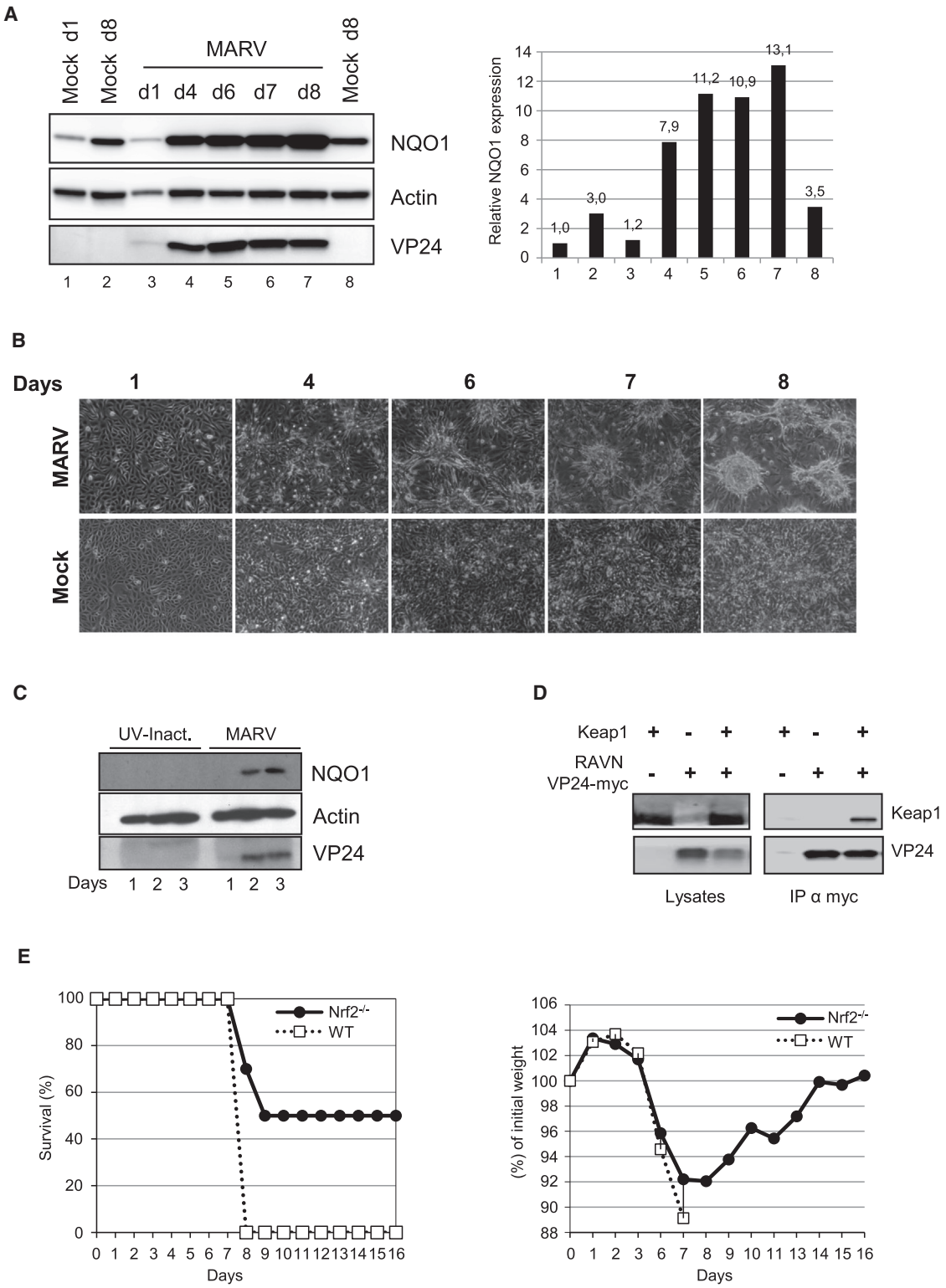

Figure 5. MARV Hijacks Nrf2-Dependent Pathway

(A–C) MARV infection results in enhanced NQO1 expression. (A and B) Vero E6 cells were either left uninfected or infected with MARV at a MOI of 2 and then were monitored for 8 days p.i. for expression of cellular NQO1 and MARV VP24 (A) and appearance of cytotoxic effects (B). Cell lysates were analyzed by western blot using VP24, NQO1, and actin antibodies. Despite apparent cytotoxic effects caused by MARV replication, comparable levels of β-actin were detected in mock- and virus-infected cells on days 1 and 8 p.i. (lanes 1 and 3, and lanes 7 and 8, respectively). In virus-infected cells, NQO1 levels increased during the course of

(legend continued on next page)

modulation. This may occur through Nrf2 displacement from the Keap1 complex or through exhaustion of existing Keap1 by MARV VP24 resulting in availability of newly synthesized Nrf2. Overall, our results strongly support the idea that MARV VP24 prevents Keap1-dependent control of Nfr2, allowing Nrf2 nuclear relocalization, and thus activation of Nrf2-dependent genes. Importantly, increased Nrf2-dependent gene expression seen in MARV-infected cells correlates with increasing VP24 synthesis during infection. Notably, over an extended period of time, MARV infection does not lead to cell damage despite apparent cytotoxic effects caused by massive viral replication. This is in sharp contrast to Ebolavirus infection, which does not activate Nrf2, resulting in ROS synthesis and early cell death.

Results with Nrf2$^{-/-}$ mice further highlights the significance of the Nrf2 pathway in Marburgvirus replication. Infection with both Ebola- and Marburgvirus is characterized by dysregulated inflammatory responses (Baize et al., 2002; Mohamadzadeh, 2009; Rubins et al., 2007). Massive infiltration of inflammatory cells to the infection site, along with elevated levels of chemokines (MIP1α, MCP1, MIP1β, MIF, and IP10), and pro- (IFN-α, tumor necrosis factor α [TNF-α], and interleukin 1β [IL-1β]) and anti-inflammatory cytokines (IL-10, IL-1RA, and IL-6) and nitric oxide and ROS release follow the infection course. Although infected cells experience oxidative exposure during infection, MARV VP24 would provide cytoprotection through sustained Nrf2 activation. Here, we show better survival and lower viral replication in Nrf2$^{-/-}$ mice compared to wild-type animals. Surviving Nrf2$^{-/-}$ mice completely clear the virus and recover from infection. We surmise that lack of VP24-induced Nrf2 pathway activation in infected Nrf2$^{-/-}$ mice likely results in elimination of these cells via host defense mechanisms. In contrast to MARV, infection of Nrf2$^{-/-}$ mice with RSV led to more severe disease compared to wild-type mouse infection (Cho et al., 2009). This may be explained by differences in pathological appearance between the two infections. RSV infection causes massive ROS release characterized by inflammation and respiratory disorders. Absence of Nrf2 resulted in augmented inflammatory reactions, severe respiratory failure and death of Nrf2$^{-/-}$ mice. MARV infection has a systemic character and the severity of the disease is determined by both virus replication rate and a host's inflammatory reactions. Perhaps loss of VP24-dependent Nrf2 pathway activation in Nrf2$^{-/-}$ animals reduces the ability of infected cells to respond to oxidative conditions caused by infiltration of inflammatory cells providing better conditions for mice survival. Survival of virus-infected cells in oxidative conditions through Nrf2 activation has also been reported for hepatitis C virus (Burdette et al., 2010) and hepatitis B virus (Schaedler et al., 2010), although the molecular mechanisms involved are unclear. Interestingly, increasing evidence indicates that certain tumor types constitutively activate the Nrf2 pathway, thus increasing their survival in the patient and enabling them to endure acute exposure to ROS-generating chemotherapeutic agents (Hayes and McMahon, 2009). Strikingly, missense mutations in Keap1 reduce Keap1 repression of Nrf2 and cause persistent Nrf2 activation. By acting continuously on the Nrf2 pathway, MARV infection causes its sustained activation perhaps in addition to oxidative stress stimulus that may contribute to host inflammatory response dysregulation.

Keap1, our identified MARV VP24 target, is involved in inflammatory response control through interaction with IkB kinase IKKb (Lee et al., 2009). IKKβ possesses the same ETGE and DLG motifs as Nrf2 and binds to Keap1 in a similar manner. Similarly, Keap1 results in IKKβ ubiquitination and degradation by the proteasome machinery. Thus, MARV VP24 binding could prevent Keap1-dependent IKKβ degradation activating the NF-κB pathway similar to the Nrf2 pathway. NF-κB controls expression of diverse processes, including inflammatory responses and cell survival. As NF-κB target genes include proinflammatory cytokines (TNFα, IL-1, and IL-6) and chemokines (MCP1 and MIP1α) upregulated during filoviral infection, we speculate that through targeting Keap1 MARV may cause persistent activation of this proinflammatory cellular pathway that could contribute to dysregulation of cellular inflammatory responses during infection. Further study will assess the role of MARV VP24 in IKKβ degradation and on the NF-κB pathway.

Although a number of publications have suggested the importance of viral targeting of the oxidative stress pathway, to our knowledge, the molecular mechanisms involved and the cellular factors targeted by viral components have not yet been clearly demonstrated (González-Gallego et al., 2011; Hosakote et al., 2011; Schaedler et al., 2010; Schwarz, 1996; Zhang et al., 2009). An intriguing possibility is that other viruses might also hijack this pathway. Future experiments will identify the Keap1 binding site on MARV VP24 and, using the reverse genetics system for MARV (Hoenen et al., 2011), test the effect of preventing VP24-Keap1 interaction on virus replication and pathogenicity. Additionally, it will be of interest to investigate whether other Kelch domain containing cellular proteins may also bind MARV VP24 and be involved in pathogenic viral replication.

In conclusion, we present a model whereby targeting Keap1, viral VP24 hijacks the Nrf2 pathway and ensures better survival of virus-infected cells despite massive host antiviral inflammatory responses to infection. Through sensing disturbances in intracellular redox balance, Keap1 can be seen as a cellular "sweeper" protein that regulates activity of various transcriptional activators, including Nrf2 and IKKβ, by targeting them for

infection. Quantification of NQO1 expression after normalization to actin levels is shown in (A), right panel. (C) 293T cells were either infected with UV-inactivated virus (nonreplicating control) or untreated MARV at equal MOI (MOI of 5). Cells were lysed at the indicated days postinfection, and samples were analyzed by western blot for expression of NQO1, MARV VP24, and actin.

(D) RAVN VP24 precipitates Keap1. Myc-tagged RAVN-VP24 (VP24) and human Keap1 were coexpressed in 293T cells. Cell lysates were collected 24 hr p.t. and assayed for protein expression and coimmunoprecipitation using myc antibody. Samples were analyzed by western blot using VP24 and Keap1 antibodies. Of note: the amino acid sequence of the Kelch domain of Keap1 is highly conserved between human and mouse, with no sequence change within the binding site for Nrf2.

(E) Nrf2$^{-/-}$ mice are less sensitive to Marburgvirus infection than wild-type animals. Mice (C57BL6 or Nrf2$^{-/-}$, n = 12 per group) were administered intraperitoneally with 1,000 pfu of mouse-adapted Marburgvirus RAVN. Mice were monitored daily for survival (left) and weight loss (right) over 16 days postadministration. The graph represents three independent experiments; error bars represents SEM.

degradation. In the presence of MARV VP24, Keap1 is no longer able to perform this function, pushing the infected cell into a state where transcriptional activation remains unchecked, altering inflammatory balance. As this virus targets immune cells responsible for limiting viral infection, the dysregulation of usually well-controlled inflammatory responses likely contributes to the pathogenesis of MARV infection.

EXPERIMENTAL PROCEDURES

Viruses

Viruses belonging to *Filoviridae* family, *Marburgvirus* genus, species Marburg virus (MARV) variant Musoke, mouse-adapted Ravn virus (ma-RAVV) variant Ravn (Warfield et al., 2009), and *Ebolavirus* genus, species *Zaire* Ebola virus (EBOV) were used.

Cell Lines, Transfection, Infection, and Plasmids

293T, Huh7, and Vero E6 cells were cultured in Dulbecco's modified Eagle's medium supplemented with 10% fetal calf serum (FCS). For transfection, cells were grown for 24 hr to a confluence of ~60%. Transfection of cells was performed using Fugene HD (Roche) or TurboFect reagent (Thermo). Cells were analyzed 24 hr posttransfection unless indicated otherwise. For infection, subconfluent Vero E6, 293T, or Huh7 cells were infected with MARV or EBOV at a multiplicity of infection (MOI) 2 or 5, respectively. One hour postinfection, inoculum was removed, and cells were left with DMEM media containing 2.5% FCS. Culture supernatants and cell lysates were collected daily as indicated. Western blot analysis was performed with corresponding antibodies (see Supplemental Experimental Procedures). Details of plasmid constructions are provided in Supplemental Experimental Procedures.

Yeast Double-Hybrid Screen

Yeast double-hybrid screen was performed as described previously (Journo et al., 2009). Details are provided in Supplemental Experimental Procedures.

Immunoprecipitation

Immunoprecipitations using μMACs separation columns and μMACS c-*myc* isolation Kit (both from MiltenyiBiotec) and EZview RedAnti-HA affinity gel (Sigma) were performed according to manufacturer's instructions (see Supplemental Experimental Procedures). Samples were analyzed by western blotting.

Immunofluorescence

Subconfluent Vero E6 cells were used for immunofluorescence analysis (see Supplemental Experimental Procedures). Pictures were taken using a Zeiss 200M fluorescent microscope. Images were analyzed by Axiovision Software (Zeiss).

Reporter Gene Assay

293T cells were transfected with the following plasmids: pHHO1-ARE-Luc or pmNQO1-ARE-Luc, phCMV-Nrf2, pSPORT6-Keap1, pRL-TK, and phCMV-MARV-VP24 using TurboFect reagent. Cells were harvested 24 hr posttransfection for measurement of luciferase activities (Renilla and Firefly) by the Dual-Glo-Luciferase kit (Promega) (see Supplemental Experimental Procedures). Data were expressed as fold induction compared to negative control.

In Vivo Studies

Wild-type or Nrf2$^{-/-}$ C57BL6 mice (n = 12 per group) were infected with mouse-adapted Marburgvirus RAVN (ma-RAVV) variant RAVN at a dose of 1,000 pfu/animal. Animals were monitored daily for weight loss and appearance of other symptoms (see Supplemental Experimental Procedures). The Institutional Animal Care and Use Committee of the United States Army Medical Research Institute of Infectious Diseases (USAMRIID) approved these studies.

SUPPLEMENTAL INFORMATION

Supplemental Information includes Supplemental Experimental Procedures, five figures, and one table and can be found with this article online at http://dx.doi.org/10.1016/j.celrep.2014.02.027.

ACKNOWLEDGMENTS

We are grateful to A.I. Cederbaum (Mount Sinai School of Medicine, New York) for the pHCMV-Nrf2 and pHHO1-Luc reporter system and to M. Yamamoto for pmNQO1-ARE-Luc. We thank L. Tafforeau, M. Lebreton, and T. Chantier for technical help with double-hybrid screening and S. Naik for reading the manuscript. We would like to acknowledge the Biosafety team members of the Jean Mérieux BSL4 facility. This work was supported by the European Union FP7 project ANTIGONE (278976), Agence Nationale de la Recherche (ANR-07-MIME-006-01), and Fondation pour la Recherche Médicale (DMI20091117323).

Received: August 2, 2013
Revised: December 13, 2013
Accepted: February 18, 2014
Published: March 13, 2014

REFERENCES

Baize, S., Leroy, E.M., Georges, A.J., Georges-Courbot, M.C., Capron, M., Bedjabaga, I., Lansoud-Soukate, J., and Mavoungou, E. (2002). Inflammatory responses in Ebola virus-infected patients. Clin. Exp. Immunol. *128*, 163–168.

Bamberg, S., Kolesnikova, L., Möller, P., Klenk, H.D., and Becker, S. (2005). VP24 of Marburg virus influences formation of infectious particles. J. Virol. *79*, 13421–13433.

Burdette, D., Olivarez, M., and Waris, G. (2010). Activation of transcription factor Nrf2 by hepatitis C virus induces the cell-survival pathway. J. Gen. Virol. *91*, 681–690.

Carvajal-Yepes, M., Himmelsbach, K., Schaedler, S., Ploen, D., Krause, J., Ludwig, L., Weiss, T., Klingel, K., and Hildt, E. (2011). Hepatitis C virus impairs the induction of cytoprotective Nrf2 target genes by delocalization of small Maf proteins. J. Biol. Chem. *286*, 8941–8951.

Cho, H.Y., Imani, F., Miller-DeGraff, L., Walters, D., Melendi, G.A., Yamamoto, M., Polack, F.P., and Kleeberger, S.R. (2009). Antiviral activity of Nrf2 in a murine model of respiratory syncytial virus disease. Am. J. Respir. Crit. Care Med. *179*, 138–150.

Feldmann, H., and Klenk, H.D. (1996). Filoviruses. In Medical Microbiology, 4th edition, S. Baron, ed. (Galveston: University of Texas Medical Branch).

Feldmann, H., Klenk, H.D., and Sanchez, A. (1993). Molecular biology and evolution of filoviruses. Arch. Virol. Suppl. *7*, 81–100.

Furukawa, M., and Xiong, Y. (2005). BTB protein Keap1 targets antioxidant transcription factor Nrf2 for ubiquitination by the Cullin 3-Roc1 ligase. Mol. Cell. Biol. *25*, 162–171.

Geisbert, T.W., Hensley, L.E., Larsen, T., Young, H.A., Reed, D.S., Geisbert, J.B., Scott, D.P., Kagan, E., Jahrling, P.B., and Davis, K.J. (2003). Pathogenesis of Ebola hemorrhagic fever in cynomolgus macaques: evidence that dendritic cells are early and sustained targets of infection. Am. J. Pathol. *163*, 2347–2370.

González-Gallego, J., García-Mediavilla, M.V., and Sánchez-Campos, S. (2011). Hepatitis C virus, oxidative stress and steatosis: current status and perspectives. Curr. Mol. Med. *11*, 373–390.

Hayes, J.D., and McMahon, M. (2009). NRF2 and KEAP1 mutations: permanent activation of an adaptive response in cancer. Trends Biochem. Sci. *34*, 176–188.

Hoenen, T., Groseth, A., de Kok-Mercado, F., Kuhn, J.H., and Wahl-Jensen, V. (2011). Minigenomes, transcription and replication competent virus-like particles and beyond: reverse genetics systems for filoviruses

and other negative stranded hemorrhagic fever viruses. Antiviral Res. *91*, 195–208.

Hosakote, Y.M., Jantzi, P.D., Esham, D.L., Spratt, H., Kurosky, A., Casola, A., and Garofalo, R.P. (2011). Viral-mediated inhibition of antioxidant enzymes contributes to the pathogenesis of severe respiratory syncytial virus bronchiolitis. Am. J. Respir. Crit. Care Med. *183*, 1550–1560.

Huang, Y., Xu, L., Sun, Y., and Nabel, G.J. (2002). The assembly of Ebola virus nucleocapsid requires virion-associated proteins 35 and 24 and posttranslational modification of nucleoprotein. Mol. Cell *10*, 307–316.

Itoh, K., Wakabayashi, N., Katoh, Y., Ishii, T., Igarashi, K., Engel, J.D., and Yamamoto, M. (1999). Keap1 represses nuclear activation of antioxidant responsive elements by Nrf2 through binding to the amino-terminal Neh2 domain. Genes Dev. *13*, 76–86.

Jaiswal, A.K. (2004). Nrf2 signaling in coordinated activation of antioxidant gene expression. Free Radic. Biol. Med. *36*, 1199–1207.

Journo, C., Filipe, J., About, F., Chevalier, S.A., Afonso, P.V., Brady, J.N., Flynn, D., Tangy, F., Israël, A., Vidalain, P.O., et al. (2009). NRP/Optineurin Cooperates with TAX1BP1 to potentiate the activation of NF-kappaB by human T-lymphotropic virus type 1 tax protein. PLoS Pathog. *5*, e1000521.

Kang, M.I., Kobayashi, A., Wakabayashi, N., Kim, S.G., and Yamamoto, M. (2004). Scaffolding of Keap1 to the actin cytoskeleton controls the function of Nrf2 as key regulator of cytoprotective phase 2 genes. Proc. Natl. Acad. Sci. USA *101*, 2046–2051.

Kobayashi, A., Kang, M.I., Okawa, H., Ohtsuji, M., Zenke, Y., Chiba, T., Igarashi, K., and Yamamoto, M. (2004). Oxidative stress sensor Keap1 functions as an adaptor for Cul3-based E3 ligase to regulate proteasomal degradation of Nrf2. Mol. Cell. Biol. *24*, 7130–7139.

Kobayashi, A., Kang, M.I., Watai, Y., Tong, K.I., Shibata, T., Uchida, K., and Yamamoto, M. (2006). Oxidative and electrophilic stresses activate Nrf2 through inhibition of ubiquitination activity of Keap1. Mol. Cell. Biol. *26*, 221–229.

Lee, D.F., Kuo, H.P., Liu, M., Chou, C.K., Xia, W., Du, Y., Shen, J., Chen, C.T., Huo, L., Hsu, M.C., et al. (2009). KEAP1 E3 ligase-mediated downregulation of NF-kappaB signaling by targeting IKKbeta. Mol. Cell *36*, 131–140.

Li, X., Zhang, D., Hannink, M., and Beamer, L.J. (2004a). Crystal structure of the Kelch domain of human Keap1. J. Biol. Chem. *279*, 54750–54758.

Li, X., Zhang, D., Hannink, M., and Beamer, L.J. (2004b). Crystallization and initial crystallographic analysis of the Kelch domain from human Keap1. Acta Crystallogr. D Biol. Crystallogr. *60*, 2346–2348.

Ligon, B.L. (2005). Outbreak of Marburg hemorrhagic fever in Angola: a review of the history of the disease and its biological aspects. Semin. Pediatr. Infect. Dis. *16*, 219–224.

Lo, S.C., Li, X., Henzl, M.T., Beamer, L.J., and Hannink, M. (2006). Structure of the Keap1:Nrf2 interface provides mechanistic insight into Nrf2 signaling. EMBO J. *25*, 3605–3617.

Ma, Q. (2013). Role of nrf2 in oxidative stress and toxicity. Annu. Rev. Pharmacol. Toxicol. *53*, 401–426.

Mahanty, S., and Bray, M. (2004). Pathogenesis of filoviral haemorrhagic fevers. Lancet Infect. Dis. *4*, 487–498.

Mateo, M., Reid, S.P., Leung, L.W., Basler, C.F., and Volchkov, V.E. (2010). Ebolavirus VP24 binding to karyopherins is required for inhibition of interferon signaling. J. Virol. *84*, 1169–1175.

Mateo, M., Carbonnelle, C., Martinez, M.J., Reynard, O., Page, A., Volchkova, V.A., and Volchkov, V.E. (2011a). Knockdown of Ebola virus VP24 impairs viral nucleocapsid assembly and prevents virus replication. J. Infect. Dis. *204* (*Suppl 3*), S892–S896.

Mateo, M., Carbonnelle, C., Reynard, O., Kolesnikova, L., Nemirov, K., Page, A., Volchkova, V.A., and Volchkov, V.E. (2011b). VP24 is a molecular determinant of Ebola virus virulence in guinea pigs. J. Infect. Dis. *204* (*Suppl 3*), S1011–S1020.

Mehedi, M., Groseth, A., Feldmann, H., and Ebihara, H. (2011). Clinical aspects of Marburg hemorrhagic fever. Future Virol. *6*, 1091–1106.

Mohamadzadeh, M. (2009). Potential factors induced by filoviruses that lead to immune supression. Curr. Mol. Med. *9*, 174–185.

Motohashi, H., Katsuoka, F., Engel, J.D., and Yamamoto, M. (2004). Small Maf proteins serve as transcriptional cofactors for keratinocyte differentiation in the Keap1-Nrf2 regulatory pathway. Proc. Natl. Acad. Sci. USA *101*, 6379–6384.

Ogura, T., Tong, K.I., Mio, K., Maruyama, Y., Kurokawa, H., Sato, C., and Yamamoto, M. (2010). Keap1 is a forked-stem dimer structure with two large spheres enclosing the intervening, double glycine repeat, and C-terminal domains. Proc. Natl. Acad. Sci. USA *107*, 2842–2847.

Padmanabhan, B., Tong, K.I., Kobayashi, A., Yamamoto, M., and Yokoyama, S. (2008). Structural insights into the similar modes of Nrf2 transcription factor recognition by the cytoplasmic repressor Keap1. J. Synchrotron Radiat. *15*, 273–276.

Pichlmair, A., Kandasamy, K., Alvisi, G., Mulhern, O., Sacco, R., Habjan, M., Binder, M., Stefanovic, A., Eberle, C.A., Goncalves, A., et al. (2012). Viral immune modulators perturb the human molecular network by common and unique strategies. Nature *487*, 486–490.

Reid, S.P., Leung, L.W., Hartman, A.L., Martinez, O., Shaw, M.L., Carbonnelle, C., Volchkov, V.E., Nichol, S.T., and Basler, C.F. (2006). Ebola virus VP24 binds karyopherin alpha1 and blocks STAT1 nuclear accumulation. J. Virol. *80*, 5156–5167.

Reid, S.P., Valmas, C., Martinez, O., Sanchez, F.M., and Basler, C.F. (2007). Ebola virus VP24 proteins inhibit the interaction of NPI-1 subfamily karyopherin alpha proteins with activated STAT1. J. Virol. *81*, 13469–13477.

Rubins, K.H., Hensley, L.E., Wahl-Jensen, V., Daddario DiCaprio, K.M., Young, H.A., Reed, D.S., Jahrling, P.B., Brown, P.O., Relman, D.A., and Geisbert, T.W. (2007). The temporal program of peripheral blood gene expression in the response of nonhuman primates to Ebola hemorrhagic fever. Genome Biol. *8*, R174.

Rushworth, S.A., MacEwan, D.J., and O'Connell, M.A. (2008). Lipopolysaccharide-induced expression of NAD(P)H:quinone oxidoreductase 1 and heme oxygenase-1 protects against excessive inflammatory responses in human monocytes. J. Immunol. *181*, 6730–6737.

Sanchez, A., Lukwiya, M., Bausch, D., Mahanty, S., Sanchez, A.J., Wagoner, K.D., and Rollin, P.E. (2004). Analysis of human peripheral blood samples from fatal and nonfatal cases of Ebola (Sudan) hemorrhagic fever: cellular responses, virus load, and nitric oxide levels. J. Virol. *78*, 10370–10377.

Schaedler, S., Krause, J., Himmelsbach, K., Carvajal-Yepes, M., Lieder, F., Klingel, K., Nassal, M., Weiss, T.S., Werner, S., and Hildt, E. (2010). Hepatitis B virus induces expression of antioxidant response element-regulated genes by activation of Nrf2. J. Biol. Chem. *285*, 41074–41086.

Schwarz, K.B. (1996). Oxidative stress during viral infection: a review. Free Radic. Biol. Med. *21*, 641–649.

Thimmulappa, R.K., Lee, H., Rangasamy, T., Reddy, S.P., Yamamoto, M., Kensler, T.W., and Biswal, S. (2006). Nrf2 is a critical regulator of the innate immune response and survival during experimental sepsis. J. Clin. Invest. *116*, 984–995.

Thimmulappa, R.K., Fuchs, R.J., Malhotra, D., Scollick, C., Traore, K., Bream, J.H., Trush, M.A., Liby, K.T., Sporn, M.B., Kensler, T.W., et al. (2007). Preclinical evaluation of targeting the Nrf2 pathway by triterpenoids (CDDO-Im and CDDO-Me) for protection from LPS-induced inflammatory response and reactive oxygen species in human peripheral blood mononuclear cells and neutrophils. Antioxid. Redox. Signal. *9*, 1963–1970.

Tong, K.I., Katoh, Y., Kusunoki, H., Itoh, K., Tanaka, T., and Yamamoto, M. (2006). Keap1 recruits Neh2 through binding to ETGE and DLG motifs: characterization of the two-site molecular recognition model. Mol. Cell. Biol. *26*, 2887–2900.

Tong, K.I., Padmanabhan, B., Kobayashi, A., Shang, C., Hirotsu, Y., Yokoyama, S., and Yamamoto, M. (2007). Different electrostatic potentials define ETGE and DLG motifs as hinge and latch in oxidative stress response. Mol. Cell. Biol. *27*, 7511–7521.

Valmas, C., and Basler, C.F. (2011). Marburg virus VP40 antagonizes interferon signaling in a species-specific manner. J. Virol. *85*, 4309–4317.

Valmas, C., Grosch, M.N., Schümann, M., Olejnik, J., Martinez, O., Best, S.M., Krähling, V., Basler, C.F., and Mühlberger, E. (2010). Marburg virus evades interferon responses by a mechanism distinct from ebola virus. PLoS Pathog. *6*, e1000721.

Volchkov, V.E., Volchkova, V.A., Ströher, U., Becker, S., Dolnik, O., Cieplik, M., Garten, W., Klenk, H.D., and Feldmann, H. (2000). Proteolytic processing of Marburg virus glycoprotein. Virology *268*, 1–6.

Warfield, K.L., Bradfute, S.B., Wells, J., Lofts, L., Cooper, M.T., Alves, D.A., Reed, D.K., VanTongeren, S.A., Mech, C.A., and Bavari, S. (2009). Development and characterization of a mouse model for Marburg hemorrhagic fever. J. Virol. *83*, 6404–6415.

Will, C., Mühlberger, E., Linder, D., Slenczka, W., Klenk, H.D., and Feldmann, H. (1993). Marburg virus gene 4 encodes the virion membrane protein, a type I transmembrane glycoprotein. J. Virol. *67*, 1203–1210.

Zhang, H.S., Li, H.Y., Zhou, Y., Wu, M.R., and Zhou, H.S. (2009). Nrf2 is involved in inhibiting Tat-induced HIV-1 long terminal repeat transactivation. Free Radic. Biol. Med. *47*, 261–268.